

Article

Influence of Different Industrial Waste Residues on Engineering Properties of High Liquid Limit Soil and Its Microscopic Mechanism

Liansheng Tang^{1,2,3,*}, Yang Chen^{1,2,4,*} , Jialun Peng^{1,2,3} and Zihua Cheng^{1,2,4}¹ School of Earth Sciences and Engineering, Sun Yat-Sen University, Zhuhai 519082, China² Southern Marine Science and Engineering Guangdong Laboratory (Zhuhai), Zhuhai 519082, China³ Guangdong Provincial Key Laboratory of Mineral Resources and Geological Processes, Guangzhou 510275, China⁴ Guangdong Provincial Key Laboratory of Geodynamics and Geohazards, Zhuhai 519082, China

* Correspondence: eestls@mail.sysu.edu.cn (L.T.); chen2267@mail2.sysu.edu.cn (Y.C.)

Abstract: High liquid limit soil has unfavorable engineering geological characteristics, such as strong disintegration, dry shrinkage and easy cracking, and easy uplift when encountering water, which will cause various problems to the engineering. At present, the relationship between the physical and mechanical properties of high liquid limit soil and the characteristics of water-soil interaction is still not clear enough. In this study, the high liquid limit soil of Zhanjiang Avenue was selected to explore the influence of different ratios of three kinds of industrial waste residues (blast furnace slag, carbide slag, and tailing sand) on the high liquid limit soil. Aiming at the common adverse engineering geological phenomena of high liquid limit soil, such as easy disintegration, dry shrinkage crack, and easy uplift in water, the effects of different industrial waste residues on the water-soil interaction characteristics of high liquid limit soil are explored through disintegration and crack tests. In addition, the effects of different kinds and ratios on the free expansion rate, pH, unconfined compressive strength, and shear strength parameters of high liquid limit soil were studied. The improvement mechanism of different industrial waste residues on the engineering properties of high liquid limit soil is discussed in terms of mineral composition and microstructure. Based on the experimental results of this study and considering the cost and engineering practice, it is suggested that the modified carbide slag optimal ratio of high liquid limit soil of Zhanjiang Avenue is 8%. The results can provide certain guidance for the improvement and application of different industrial waste residues on high liquid limit soil to achieve the effect of sustainable development.

Keywords: industrial waste residues; high liquid limit soil; engineering properties; water-soil interaction characteristics



Citation: Tang, L.; Chen, Y.; Peng, J.; Cheng, Z. Influence of Different Industrial Waste Residues on Engineering Properties of High Liquid Limit Soil and Its Microscopic Mechanism. *Buildings* **2023**, *13*, 235. <https://doi.org/10.3390/buildings13010235>

Academic Editor: Ahmed Senouci

Received: 20 December 2022

Revised: 7 January 2023

Accepted: 12 January 2023

Published: 14 January 2023



Copyright: © 2023 by the authors. Licensee MDPI, Basel, Switzerland. This article is an open access article distributed under the terms and conditions of the Creative Commons Attribution (CC BY) license (<https://creativecommons.org/licenses/by/4.0/>).

1. Introduction

Under the geological environment conditions such as warm climate and abundant rainfall, the soil is usually highly weathered, resulting in a large proportion of fine particles in the soil, which is easy to form high liquid limit soil. The engineering properties of high liquid limit soil are relatively special. It has the characteristics of high liquid limit, high plasticity index, and high expansion rate. It also has unfavorable engineering geological characteristics such as strong disintegration, susceptibility to dry shrinkage cracking, and being easy to uplift when encountering water [1–4]. When the water content of the high liquid limit soil is high, it is usually bonded into a large mass with high plasticity, and when the water content is low, the block of high liquid limit soil is hard. If the high liquid limit soil is directly used in engineering without improvement, the soil is often difficult to be compacted during construction and prone to the phenomenon of “spring soil”. It is worth noting that in the hot and rainy climate, the variation range of soil moisture content is

large, and water is a common factor inducing engineering geological disasters, and the high liquid limit soil water has a greater impact on its engineering characteristics [5,6]. When the rainwater penetrates into the high liquid limit soil, the soil will produce expansion force. When the expansion force is too large, the internal structure of the high-liquid-limit soil will be damaged, and the phenomenon of disintegration will occur, which will cause engineering problems such as road sag, collapse, and engineering landslide. The high liquid limit soil is prone to dry shrinkage cracking when it is dry and dehydrated. It is easy to form cracks in the subgrade and pavement, which will destroy the deformation and strength characteristics of the soil [7,8]. Moreover, the high liquid limit soil has strong hydrophilicity, water retention, and capillary effect. Under the action of capillary water, the soil volume expands and upward uplift, which brings some safety problems to engineering construction and geological environment. These characteristics often cause serious damage to engineering construction and engineering geological environment in high liquid limit soil areas and great losses to people's property.

In view of the adverse engineering geological characteristics of high liquid limit soil, such as strong disintegration, susceptibility to dry shrinkage cracking, and being easy to uplift in case of water, it is necessary to adopt appropriate means to improve it to meet the requirements of the practical engineering. Appropriate soil improvement methods can improve the engineering properties of the soil, so that the defective indexes of the problem soil can reach the qualified standard [9–12]. Soil improvement methods are mainly divided into physical improvement and chemical improvement. However, physical improvement, such as dynamic compaction, will produce large noise and vibration, and may cause damage to the slope and surrounding buildings [13–16]. The chemical improvement of soil is usually to add an improver to the soil. The improver can directly react with the water or mineral components in the soil to form a new cement, so as to fill the pores between the soil and make the soil more compact [17–21]. Chemical improvement has received more and more attention because of its advantages such as convenient construction and stable soil performance [22–25]. Many scholars have carried out a lot of research on soil improvement and have achieved many important results [26–30]. Kong et al., [31] used lignin to improve the engineering properties of high liquid limit soil, and found that lignin can improve its engineering properties mainly through ion exchange, hydrogen bond, covalent bond, and electrostatic attraction. Sun et al., [32] found that sand mixing can significantly reduce the liquid limit and plasticity index of high liquid limit soil and improve the CBR value. Wang et al., [2] used inorganic materials (cement, quicklime, and fly ash) and vulcanized oil to improve the high liquid limit soil. The strength of the high liquid limit soil can be significantly improved by adding only inorganic materials, while the water stability characteristics of the high liquid limit soil can be improved by adding vulcanized oil, and the optimal mixing ratio of the modified materials is obtained. Que et al., [3] used CSIS and CLIS composite materials to improve the high liquid limit soil, so that the unconfined compressive strength and crack resistance of the soil are better than that of cement alone. Most scholars only study some parameters of high liquid limit soil, but the undesirable characteristics of high liquid limit soil are not limited to this. High liquid limit soil has strong disintegration, easy to dry shrinkage crack, and easy to uplift in case of water. Therefore, it is necessary to further systematically study the water-soil interaction characteristics (disintegration and crack) of high liquid limit soil and make targeted improvement. At the same time, the relationship between the physical and mechanical properties of high liquid limit soil and the characteristics of water-soil interaction is still not clear enough.

At present, the most commonly used soil chemical improvers are lime and cement, but the traditional lime and cement ash also have some shortcomings [33,34]. Although their improvement effect is very good, lime and cement are resource materials with relatively high cost [35]. Moreover, it consumes a lot of energy in exploiting raw materials and produces a large amount of dust and harmful gases in the production process, which will have a certain impact on the environment [36–39]. At present, there is a huge amount

of industrial waste residues in China. Improper disposal will not only increase the cost, but also cause a certain degree of resource waste and environmental pollution [40–42]. Carbide slag can react with soil components to make the soil structure more compact, thus improving the engineering properties of the soil. Blast furnace slag in concrete admixtures and tailing sand with similar physical and chemical properties to building materials are common and optional modified materials. They have a large stockpile in industrial links and are harmful to the environment. There are a lot of blast furnace slag, carbide slag, and tailing sand in Zhanjiang. Therefore, these three kinds of industrial waste residues are selected for soil improvement. The use of industrial waste residues to improve the high liquid limit soil cannot only reduce the use of resource materials to reduce the cost. At the same time, it also provides a way to realize resource and harmless treatment of industrial waste residues, and finally achieve the purpose of waste utilization and turning waste into treasure.

High liquid limit soils are widely distributed in warm and rainy regions all over the world. To prevent the bad engineering characteristics of high liquid limit soil from causing serious damage to the project, it is necessary to improve the engineering properties of high liquid limit soil. Under the background of engineering practice, the high liquid limit soil of Zhanjiang Avenue in Guangdong Province is used in the test to explore the influence of three kinds of industrial waste residues (blast furnace slag, carbide slag, and tailing sand) with different ratio (0%, 4%, 8%, 12%, and 16%) on the free expansion rate, pH, unconfined compressive strength, shear strength, disintegration and crack of the high liquid limit soil. Finally, the improvement mechanism of different industrial waste residues on high liquid limit soil was explained from the perspective of mineral composition and microstructure by combining X-ray diffraction (XRD) and scanning electron microscope (SEM).

2. Materials and Methods

2.1. Materials

2.1.1. High Liquid Limit Soil

The high liquid limit soil samples in this study are taken from Zhanjiang Avenue, Zhanjiang City, Guangdong Province. The soil in natural state is yellowish brown. The soil grading curve is shown in Figure 1. In the original soil sample of this test, the proportion of soil particles with particle size < 0.075 mm reaches 77.6%, and the content of fine particles is relatively large. The fundamental physical parameters of high liquid limit soil are shown in Table 1.

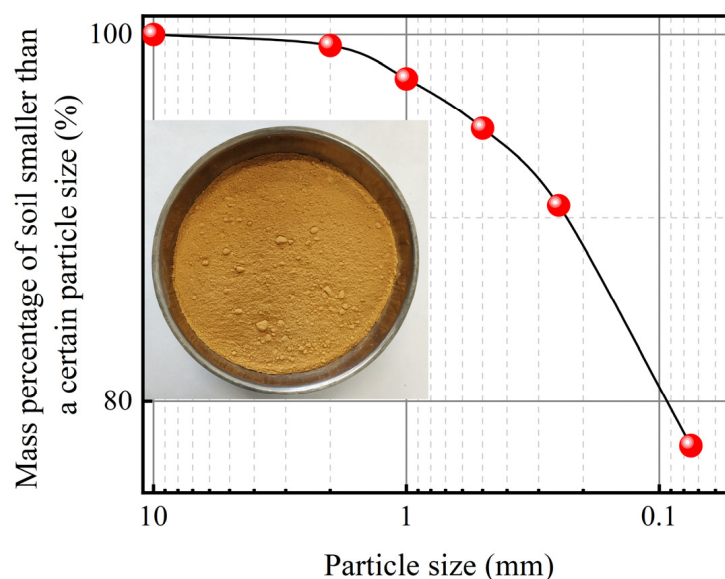


Figure 1. Grading curve of original soil sample.

Table 1. Fundamental physical parameters of high liquid limit soil.

Natural Moisture Content (%)	Liquid Limit (%)	Plastic Limit (%)	Plasticity Index (%)	pH
31.8	53.1	23.5	29.6	6.1

2.1.2. Industrial Waste Residues

In view of the undesirable characteristics of high liquid limit soil, such as high expansion rate, strong disintegration, easy to dry shrinkage crack, and easy to uplift in case of water, the influence of three kinds of industrial waste powders on high liquid limit soil was mainly considered. Blast furnace slag powder is white and its particle surface is smooth and dense; The color of carbide slag powder is gray, with pungent smell; The surface of tailing sand powder particles is brown. In the test, the particle size of blast furnace slag powder is less than 0.013 mm, carbide slag powder is less than 0.075 mm, and tailing sand powder is less than 0.125 mm. The chemical elements of three industrial waste residues are shown in Table 2.

Table 2. Chemical composition of three industrial wastes.

Industrial Waste Residues	SiO ₂ /%	CaO/%	Al ₂ O ₃ /%	Fe ₂ O ₃ /%	MgO/%
Blast furnace slag	32.5	40.7	15.8	0.15	8.7
Carbide slag	5.5	82.5	4.8	0.8	0.4
Tailing sand	58.3	13.2	5.2	10.2	1.8

- (1) Blast furnace slag: blast furnace slag is composed of gangue, flux, and other impurities that cannot enter pig iron in the process of blast furnace ironmaking and has more irregular pore structure. Blast furnace slag is mainly used as concrete admixture, cement mixture, and road construction in the construction industry [43]. Its main components are silica, calcium oxide, and magnesium oxide, among which silica and some metal oxides can provide reactants for volcanic ash reaction, so as to play a role in soil improvement [44].
- (2) Carbide slag: carbide slag is a solid waste residue generated after the reaction of carbide and water to obtain acetylene gas. Its main component is Ca(OH)₂ and contains a small amount of silica [45]. Carbide slag is highly alkaline, and the accumulation of a large amount of carbide slag will cause soil calcification. The composition of carbide slag is similar to that of hydrated lime, but has a larger specific surface area and is more reactive than hydrated lime. Moreover, carbide slag contains a certain amount of SiO₂. Compared with the improvement of lime, carbide slag will not produce dust phenomenon during the improvement of construction, and the raw material is only one tenth of the economy of lime. At the same time, the environmental pollution caused by carbide slag accumulation in the open air is solved.
- (3) Tailing sand: tailing sand is a kind of solid waste residue left after beneficiation, and random accumulation will cause certain pollution to the environment. Its physical and chemical properties are similar to those of building materials, and it can be used for concrete pipe piles and modified mortar. The main components of tailing sand are silica, alumina, and magnesium oxide, whose mineral composition is similar to that of natural sand. Therefore, tailing sand can play a role in replacing natural sand.

2.2. Sample Preparation

The soil improvement test conditions of different industrial waste residues with different ratios are shown in Table 3. Dry the high liquid limit soil and grind it fine, then pass a 2 mm screen. The three kinds of industrial waste residues were mixed with different ratios of 0%, 4%, 8%, 12%, and 16% (mass of industrial waste residue divided by mass of soil sample), and the water content of soil sample was prepared with 18% water content. After the waste residue and soil were thoroughly stirred, the material was stuffy for 24 h, and

the dry density of soil sample was controlled to be 1.62 g/cm^3 . Unconfined compressive strength tests were performed by compaction method, and direct shear and disintegration tests were performed by static compression method. The samples were cured for 3 days at room temperature and then tested.

Table 3. Soil improvement test conditions of different industrial waste residues with different ratios.

Soil Sample No.	Type of Waste Residue	Ratio (%)
0	/	0
1	Blast furnace slag	4
2	Blast furnace slag	8
3	Blast furnace slag	12
4	Blast furnace slag	16
5	Carbide slag	4
6	Carbide slag	8
7	Carbide slag	12
8	Carbide slag	16
9	Tailing sand	4
10	Tailing sand	8
11	Tailing sand	12
12	Tailing sand	16

2.3. Experimental Method

The soil improvement test process is shown in Figure 2, which is mainly divided into physical and chemical tests, mechanical tests, water-soil interaction tests, mineralogical and microscopic tests. Physical and chemical tests include free expansion rate and pH tests. Mechanical tests mainly include unconfined compressive strength and direct shear tests. Water-soil interaction tests include disintegration and crack tests. Mineralogical and microscopic tests include XRD and SEM.

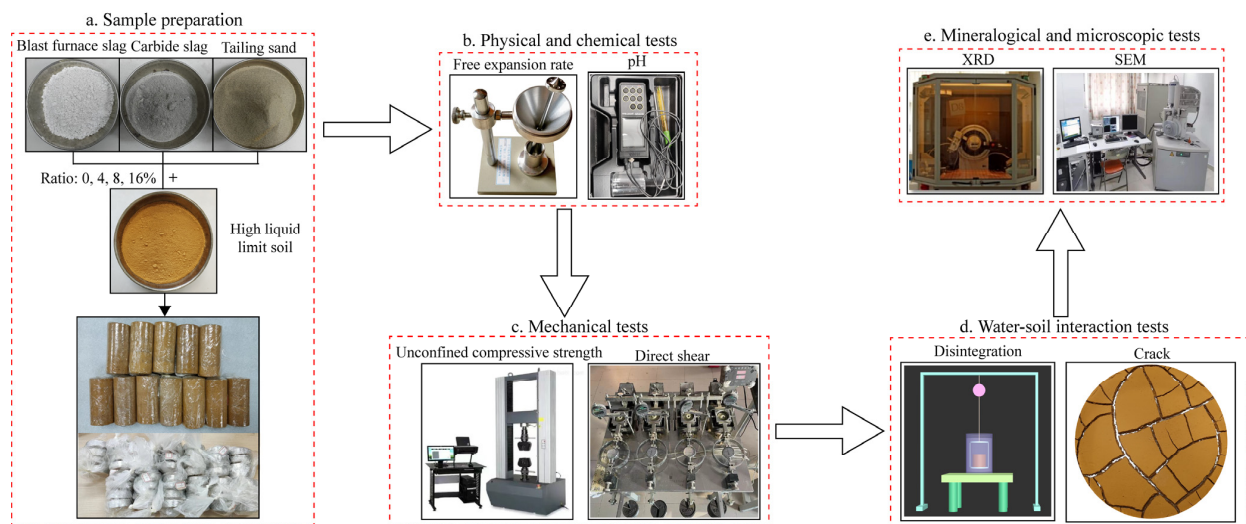


Figure 2. Schematic diagram of test flow. (a) Sample preparation (b) Physical and chemical tests (c) Mechanical tests (d) Water-soil interaction tests (e) Mineralogical and microscopic tests.

2.3.1. Physical and Chemical Tests

According to the standard GB/T50123-2019, the soil samples were crushed and passed through a 0.5 mm sieve. The soil sample is weighed in the soil cup and poured into the measuring cylinder containing some water (Figure 2b). After the soil surface is stabilized, calculate the free expansion rate of the soil. The free expansion rate of soil is the volume of soil sample increased in water divided by the initial volume of soil sample. The pH of soil was measured by potentiometric method (Figure 2b).

2.3.2. Mechanical Tests

The mechanical tests of soil samples shall be carried out according to the standard GB/T50123-2019 (Figure 2c). MTS universal testing machine was used to test the unconfined compressive strength of soil samples. The loading rate was set at 1.6 mm/min. In the direct shear test, ZJ strain controlled direct shear instrument was used for rapid shear test. Four groups of normal stresses (100, 200, 300, and 400 kPa) were set during the test. The test shear amount was 6 mm and the shear rate was 0.8 mm/min.

2.3.3. Water-Soil Interaction Tests

The disintegration test adopts the high cutting ring sample (the height is 40 mm), and the disintegration test adopts the self-developed disintegration instrument, which is mainly composed of tension meter, disintegration cylinder, and disintegration bracket [32]. The prepared disintegration sample is weighed and placed on the bracket, and the nylon rope is used to connect the disintegration bracket and the tension meter [46]. Then the disintegration bracket containing the sample was slowly immersed into the disintegration cylinder containing water, and the tension meter data were recorded by the camera during the whole process (Figure 2d) [47].

A round glass dish with a diameter of 15 cm was uniformly selected for the crack test container. A 200 g soil sample was added to the glass dish, and water was added to configure it into a saturated slurry with 100% water content. The mud was evenly stirred with a glass rod and left for 24 h. During the test, the soil was placed in a constant temperature and dry environment of 60 °C, and when the soil did not change, the soil cracking was over (Figure 2d).

2.3.4. Mineralogical and Microscopic Tests

The Empyrean XRD instrument was used to determine the mineral composition of the soil samples. The starting angle of the test was 10°, the ending angle was 80°, the step width was 0.02°, and the sampling time was 0.05 s (Figure 2e). The soil samples were lyophilized to prepare SEM microscopic soil samples, and the microstructure of the soil samples was observed by Quanta 650 scanning electron microscope (Figure 2e). The PCAS software developed by [48] was used to analyze the morphological characteristics of the SEM images, such as pores and particles.

3. Results Analysis

3.1. Characteristics of Free Expansion Rate of Different Waste Residues Soils

Figure 3 shows that the free expansion rate of plain soil is 49%, and carbide slag has the best improvement effect. When the carbide slag ratio is only 4%, the free expansion rate of soil decreases to 23%. With the increase of carbide slag ratio, the free expansion rate of soil decreases continuously. When the carbide slag ratio exceeds 8%, the downward trend of free expansion rate starts to slow down. Considering the cost and improvement effect, it is considered that the carbide slag ratio of 8% is the optimal ratio. The main component of carbide slag is $\text{Ca}(\text{OH})_2$. Ca^{2+} can be precipitated in water, which can make the electric double layer of high liquid limit soil thin. Therefore, carbide slag can effectively reduce the free expansion rate of high liquid limit soil. The industrial waste residue with the next best improvement effect is tailing sand. When tailing sand ratio increases to 16%, the free expansion rate of high liquid limit soil decreases to 27%, and the downward trend is relatively stable. This is because the tailing sand is mainly quartz, and its mineral composition is stable in chemical properties. When tailing sand is added to the high liquid limit soil, the content of clay minerals in the soil decreases, which leads to the reduction of the free expansion rate of the high liquid limit soil. Blast furnace slag has the weakest improvement effect on the free expansion rate. The mechanism of reducing the free expansion rate of high liquid limit soil is similar to that of tailing sand, which reduces the free expansion rate by reducing the clay mineral content in high liquid limit soil.

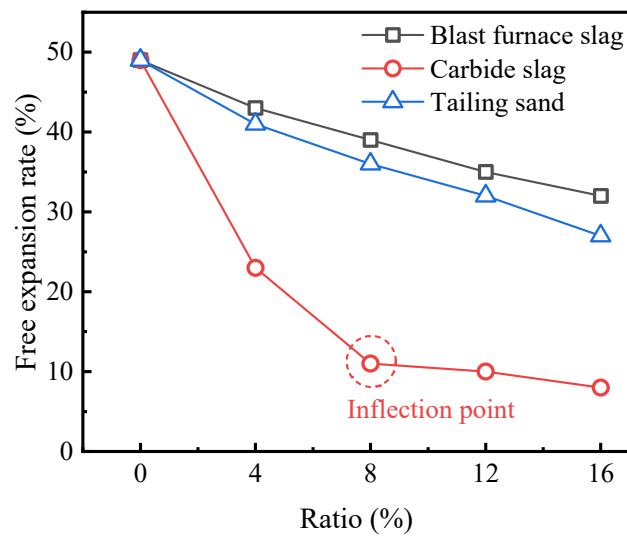


Figure 3. Free expansion rate of different waste residues soils.

3.2. Characteristics of pH of Different Waste Residues Soils

The industrial waste residue is usually acidic or alkaline. When the industrial waste residues with acid and alkaline contact with the soil, chemical reaction will occur with soil, which will affect the engineering characteristics of the soil. As shown in Figure 4, the pH of plain soil is 6.1, which is weakly acidic, and the pH of soil increases after adding three kinds of industrial waste residues with different ratio. The pH of soil increases with the increase of blast furnace slag ratio. When the blast furnace slag ratio is 16%, the pH of soil is 9.2. The main component of carbide slag is $\text{Ca}(\text{OH})_2$, which is a strong alkali substance, so the soil alkalinity increases rapidly with the increase of carbide slag ratio. When the carbide slag ratio is 4%, the soil pH is 12.2, but when the carbide slag ratio is greater than or equal to 8%, the soil pH is always 12.4, at this time, the ratio of $\text{Ca}(\text{OH})_2$ in the solution has reached the saturation state. The soil pH after adding carbide slag is high, and the soil is strongly alkaline, which may have a certain impact on the environment. Therefore, attention should be paid to the impact of strong alkali on the environment when using carbide slag to improve the soil. The pH of the soil improved by tailing sand is in the range of 7.1–7.4. The improvement of tailing slag has little impact on the pH of the soil, which is relatively friendly to the environment.

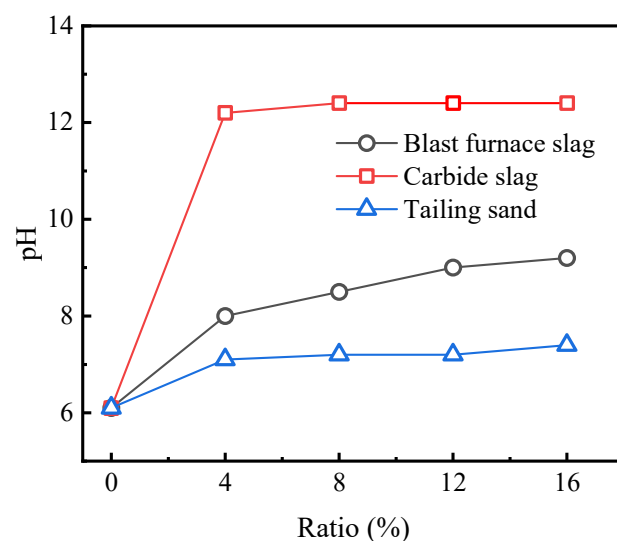


Figure 4. pH of different waste residues soils.

3.3. Characteristics of Unconfined Compressive Strength of Different Waste Residues Soils

It can be seen from Figure 5a–c that the stress-strain curves of soil samples are strain softening type. The failure modes of soil samples can be divided into shear failure and coupled tension-shear failure. The splitting failure zone of the soil sample under uniaxial compression runs through the top and bottom of the sample, and the failure surface is rough, resulting in a large number of large pieces of debris, and some of the soil samples also have compression cones.

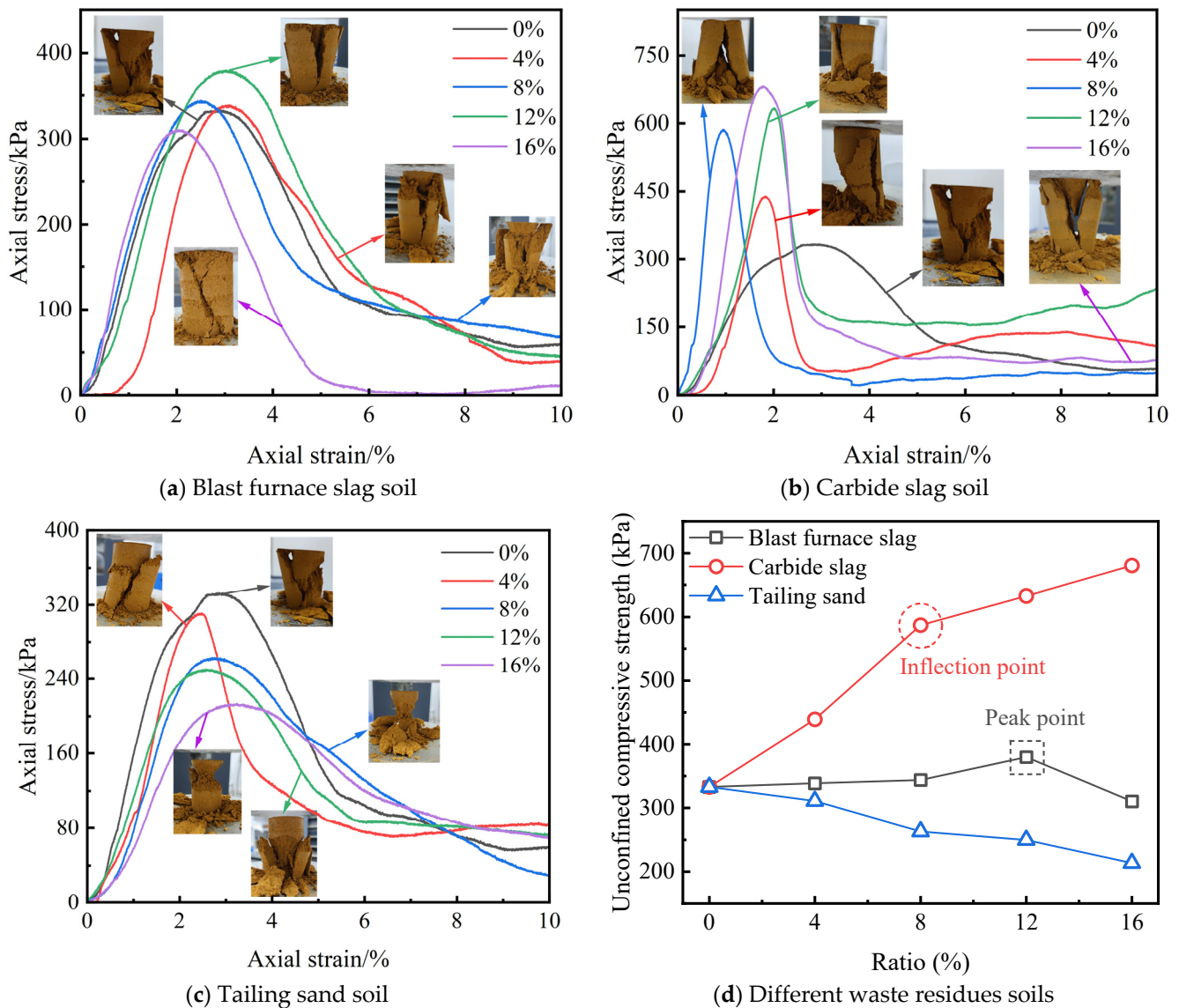


Figure 5. Unconfined compressive strength of different waste residues soils.

As shown in Figure 5d, carbide slag has the best effect on the improvement of unconfined compressive strength of high liquid limit soil. With the increase of carbide slag ratio, the unconfined compressive strength of soil also increases. When carbide slag ratio is 8%, the unconfined compressive strength of the soil sample is the inflection point, and the increment of the unconfined compressive strength of the soil sample is greater than that of other ratios. Considering the cost and improvement effect, it is considered that the carbide slag ratio of 8% is the optimal ratio. With the increase of blast furnace slag ratio, the compressive strength of high liquid limit soil increases first and then decreases. When the ratio of blast furnace slag is 12%, the peak point is reached. In general, the increase of unconfined compressive strength of modified soil is small. Blast furnace slag is a kind of

high-quality geopolymer cementitious material. Theoretically, adding blast furnace slag to high liquid limit soil will greatly improve the strength of soil, but the improvement effect is not obvious when adding blast furnace slag alone. It is speculated that there is a relatively stable protective film (silica-oxygen network structure layer) on the surface of blast furnace slag, which leads to relatively stable properties of blast furnace slag and difficult to hydrate. The unconfined compressive strength of blast furnace slag decreases when the ratio of modified soil is 16%. This is because the strength of hydration increase of blast furnace slag is less than the strength of clay mineral content decrease of high liquid limit soil. The unconfined compressive strength of high liquid limit soil decreases gradually with the increase of tailing sand ratio. This is because the tailing sand itself is stable, and the dry density and water content of the soil sample are unified in this industrial waste residue soil improvement sample preparation. Firstly, the density of tailing sand is high, and the volume of tailing sand with the same mass is much smaller than the volume of soil particles with the same mass, which leads to the reduction of the density of tailing sand modified soil. Secondly, as the proportion of tailing sand in the soil sample increases, the content of clay minerals decreases, which leads to the decreasing trend of unconfined compressive strength of the modified soil with tailing sand.

3.4. Characteristics of Shear Strength of Different Waste Residues Soils

It can be seen from Figure 6 that with the increase of blast furnace slag ratio, the shear strength at normal stress of 400 kPa increases first and then decreases, and the ratio of 12% is the peak point, which is consistent with the change law of unconfined compressive strength. Under the same normal stress, the shear strength of carbide slag increases with the increase of carbide slag ratio. When the tailing sand ratio increases, the shear strength of the soil presents a downward trend. When the normal stress is 100 kPa, the shear strength of the tailing sand decreases greatly.

Figure 7 shows that adding blast furnace slag to the high liquid limit soil generally reduces the cohesion of soil. The cohesion of blast furnace slag soil decreases twice and increases once. When the ratio of blast furnace slag is less than 8%, the cohesion of soil presents a downward trend. However, when the ratio of blast furnace slag is 12%, the cohesion of soil increases to a certain extent, but its value is still less than that of plain soil. When the ratio of blast furnace slag is 16%, the cohesion of soil continues to decrease. The internal friction angle of the soil with different ratios of blast furnace slag also increased first and then decreased. When the ratio of blast furnace slag was 8%, the internal friction angle of the soil reached the peak, and the internal friction angle of the high liquid limit soil with blast furnace slag was greater than that of the plain soil. When blast furnace slag is added to the high liquid limit soil, the potential activity of blast furnace slag cannot be excited. The addition of blast furnace slag will lead to the relative reduction of clay mineral content in the high liquid limit soil, thus reducing the cohesion of the soil. The form of blast furnace slag is mainly irregular granular, so the internal friction angle provided by soil mixed with blast furnace slag is greater than that of plain soil. For the improvement of carbide slag, with the increase of carbide slag ratio, the cohesion and internal friction angle of high liquid limit soil increase. This is because the main component of carbide slag is $\text{Ca}(\text{OH})_2$, which will generate calcium silicate hydrate, calcium aluminate hydrate, and calcium carbonate through volcanic ash reaction (Equations (1) and (2)) and carbonation reaction (Equation (3)) with mineral components in the soil [49]. The increase of tailing sand ratio will decrease the cohesion of soil and increase the internal friction angle. Carbide slag and tailing sand can increase the internal friction angle of soil. Tailing sand is an inert material, and its improvement method belongs to physical improvement. The addition of tailing sand can reduce the clay mineral content of high liquid limit soil, thus reducing the cohesion of soil. The occluding effect between tailing sand and soil particles will increase the internal friction angle of high liquid limit soil. In conclusion, carbide slag has the best improvement effect on high liquid limit soil, and can better improve its unconfined compressive strength and shear strength indexes. The improvement effect of blast furnace

slag is not obvious, tailing sand will reduce the unconfined compressive strength and shear strength of soil.

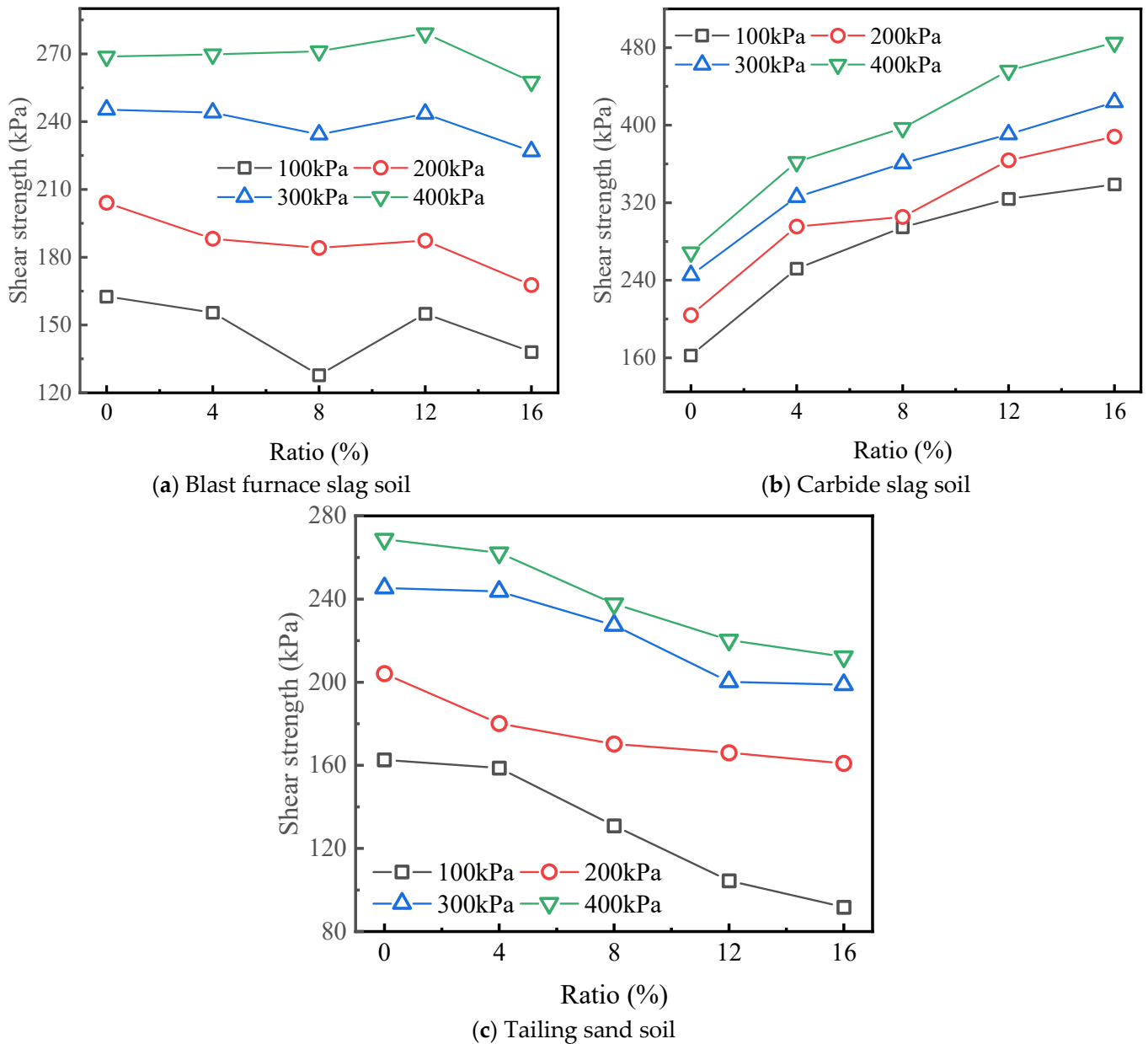


Figure 6. Change curves of shear strength of different waste residues soils.

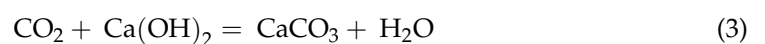
Calcium silicate hydrate



Calcium aluminate hydrate



Calcium carbonate



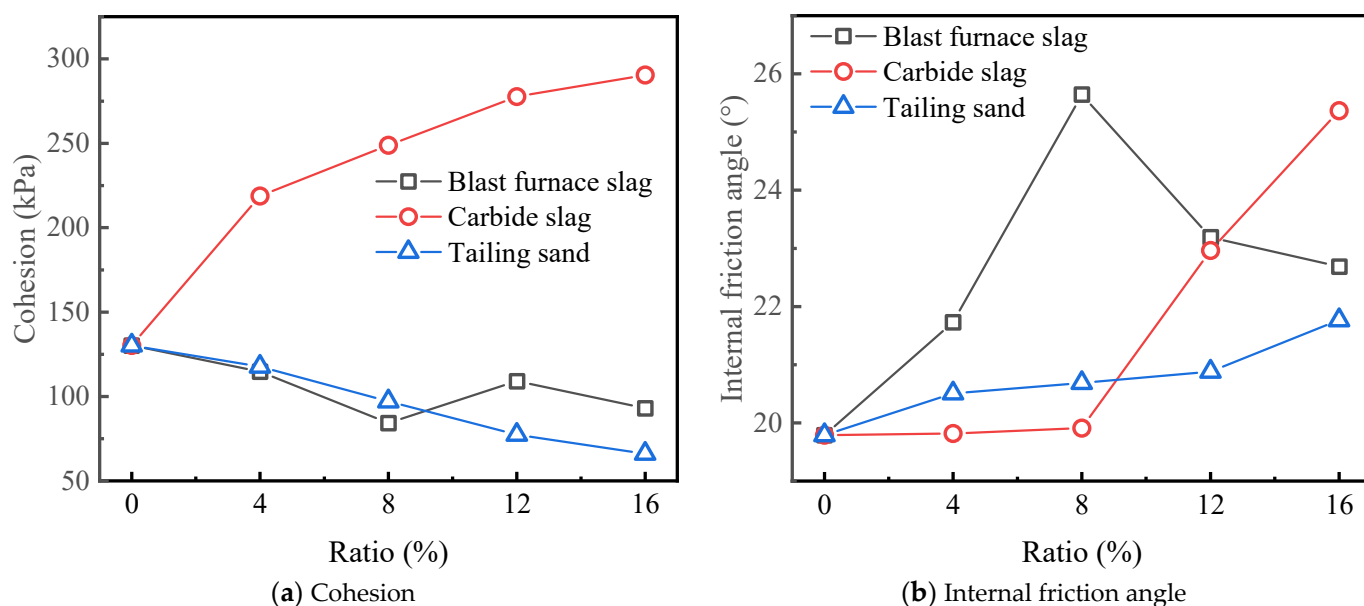


Figure 7. Change curves of cohesion and internal friction angle of different waste residues soils.

3.5. Disintegration Characteristics of Different Waste Residues Soils

As shown in Figure 8, the disintegration curve of high liquid limit soil is mainly divided into two types: near-linear type and S-type, and the S-type disintegration curve has obvious stages. The disintegration curve of blast furnace slag and tailing sand modified soil is nearly linear, which is due to its strong disintegration. The disintegration curve of carbide slag modified soil is S-type, which is due to the weak disintegration of this kind of soil. The soil sample of S-type disintegration curve is in the initial disintegration stage at the early stage of disintegration. At this stage, the soil is in the water softening stage, and the rapid decrease of soil strength leads to the increase of soil disintegration velocity. The middle stage of the S-type disintegration curve is the stable disintegration stage, at which time the disintegration velocity of the soil is approximately unchanged. The late stage of the S-type disintegration curve is the end disintegration stage, at which time the disintegration velocity of the soil sample decreases sharply until it no longer disintegrates. As shown in Figure 8a, the more blast furnace slag ratio in soil, the shorter the complete disintegration time of the modified soil. The slope of the disintegration curve of carbide slag is significantly smaller than that of plain soil (Figure 8b). With the increase of carbide slag ratio, the complete disintegration time of soil becomes longer and the final disintegration rate decreases. Figure 8c shows that when tailing sand ratio is 4%, the complete disintegration time of tailing sand is longer than that of plain soil. When the tailing sand ratio is 8%, 12% and 16%, the disintegration curves of soil are close to each other, indicating that the greater the tailing sand ratio is, the shorter the complete disintegration time is.

As shown in Figure 8d, the disintegration time is 265 s when the ratio of blast furnace slag is 4%. When the ratio of blast furnace slag is increased to 8%, the disintegration velocity increases rapidly and the complete disintegration time is rapidly shortened to 92 s. When the ratio increases to 12% and 16%, the decline of the complete disintegration time is small. In general, adding blast furnace slag to the high liquid limit soil will make the soil disintegration stronger. When the ratio exceeds 8%, the difference of soil disintegration becomes smaller. The phenomenon of blast furnace slag accelerating the disintegration of high liquid limit soil is firstly because the hydration degree of single-mixing blast furnace slag is very small, and the content of clay minerals in the soil decreases when the blast furnace slag is added to the plain soil. The second reason is that the blast furnace slag is a mixture with many irregular pore structures, which leads to the serious pore bipolarization of soil, which leads to the enhancement of the disintegration of blast furnace slag soil.

The disintegration time of the soil with 4% carbide slag is 425 s. With the increase of the ratio of carbide slag, the disintegration time of the soil steadily increases. When the ratio of 16% carbide slag is added, the disintegration time of the soil increases to 1257 s. This is because the increase of the cohesion of the modified soil with carbide slag can reduce the disintegration of the soil. Generally speaking, the stronger the cohesion of the soil, the weaker the disintegration, and the stronger the swelling of the soil, the stronger the disintegration [32]. The reason for the decline of disintegration at 4% tailing sand is presumed to be that the influence of the weakening of swelling on disintegration exceeds that of the weakening of cohesion, thus leading to the weakening of disintegration at this time. When the ratio of tailing sand exceeds 4%, the weakening cohesion plays a dominant role in the disintegration, so the disintegration of soil becomes stronger with the increase of the ratio.

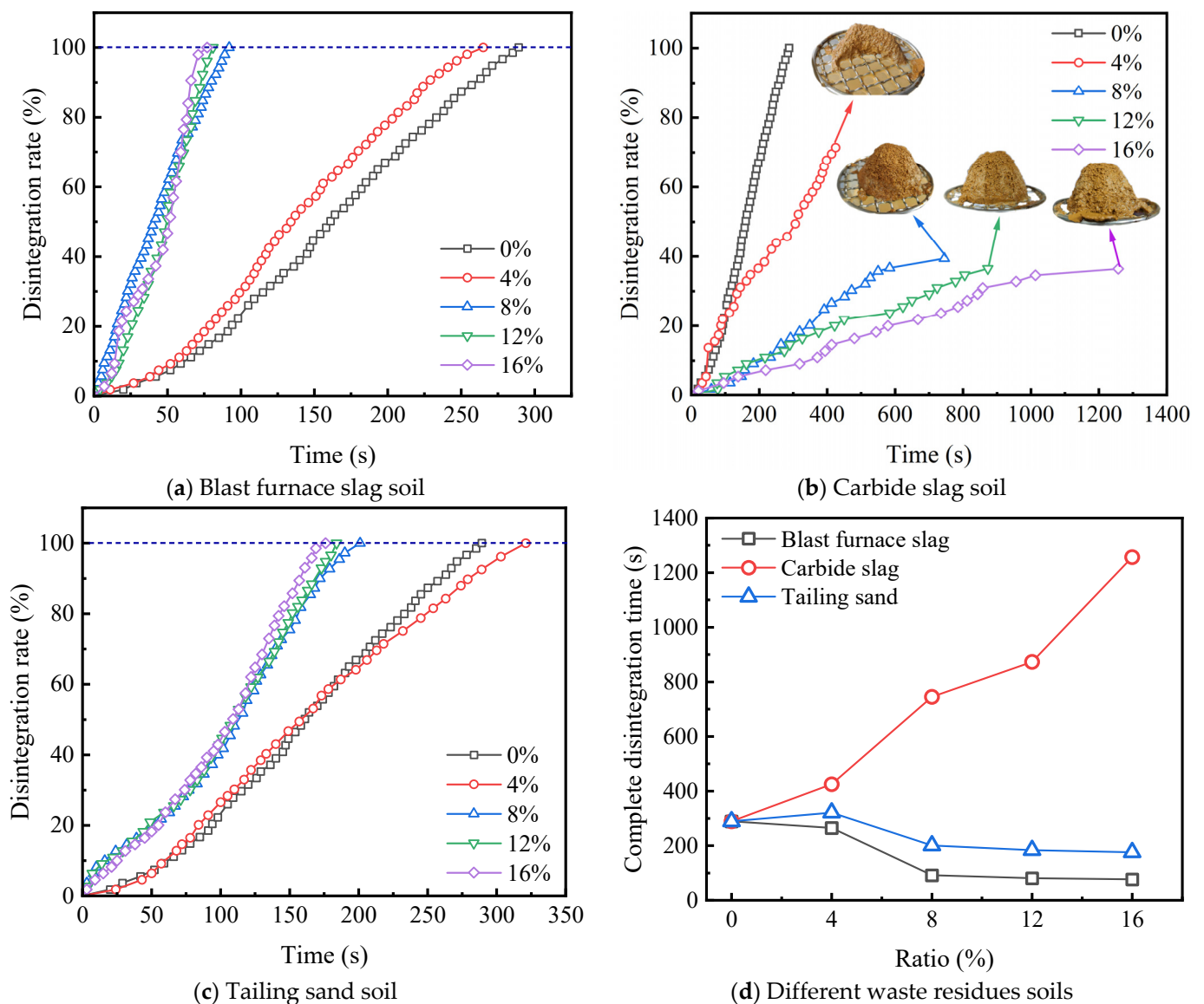


Figure 8. Disintegration curves of different waste residues soils.

Among the 13 kinds of disintegrated soil samples, only the soil with carbide slag has a final disintegration rate less than 100%, while the rest of the soil samples completely disintegrate in a short time, indicating that carbide slag can significantly reduce the disintegration of high liquid limit soil. With the ratio of carbide slag increasing to 4%, 8%, 12%, and 16%, the final disintegration rates of soil are 71.4%, 39.4%, 36.5%, and 36.4%,

respectively. Considering the cost and improvement effect, the optimal ratio of carbide slag improvement is 8%. The disintegration of carbide slag soil is also different from that of other soil samples. After the immersion of other soil samples, the soil disintegration was mostly in the form of powder soil particles scattered around and the solution was relatively cloudy, indicating that the dispersion of this kind of soil was very strong. However, the disintegration surface of the soil after the carbide slag soil is soaked in water is mostly in blocks or flakes and the solution is relatively clear, which indicates that the carbide slag reduces the disintegration of the soil sample and also effectively reduces the dispersion of the soil. Another evidence to prove the stronger interaction between carbide slag with clay, compared to the other two waste residues.

3.6. Crack Characteristics of Different Waste Residues Soils

As shown in Figure 9, the crack rate of plain soil is 11.7%. Carbide slag is the industrial waste residue with the best improvement of dry shrinkage characteristics of high liquid limit soil. The high liquid limit soil with carbide slag has the smallest crack rate, and the crack rate is 0.82% when the ratio is 4%. This is because calcium hydroxide is abundant in carbide slag. When carbide slag is immersed in water, the concentration of Ca^{2+} in water will rise, and the development of electric double layer of clay minerals will be inhibited, thus the formation of soil cracking will be inhibited. With the increase of tailing sand from 4% to 16%, the crack rate of soil decreases steadily. When the ratio of tailing sand is 16%, the crack rate of soil is 8.2%. Because the chemical properties of tailing sand are relatively stable, the incorporation of tailing sand reduces the content of clay minerals in the high liquid limit soil, thus reducing the crack rate of soil. However, the improvement effect of blast furnace slag alone is the worst, and there is no obvious law between the ratio of blast furnace slag and the crack rate of soil.

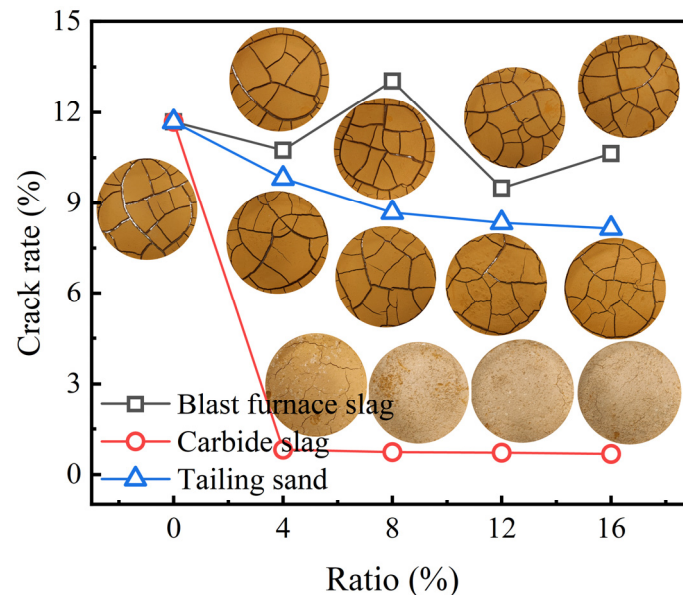


Figure 9. Crack rate of different waste residues soils.

3.7. Mineral Composition of Different Waste Residues Soils

Figure 10 shows that the main mineral components of high liquid limit soil are quartz, montmorillonite, kaolinite and illite. The single addition of blast furnace slag has little effect on the mineral composition of the soil. When the ratio of blast furnace slag is 16%, there is only one diffraction peak of quartz more than other soil samples (Figure 10a). The mineral composition of the modified soil from blast furnace slag does not change much, so the physical and mechanical properties of the modified soil do not change much. Figure 10b shows that the height and area of the diffraction peak of calcite increase gradually with

the increase of the ratio of carbide slag in high liquid limit soil. The content of calcite in carbide slag soil increases gradually, which is the reason for the improvement of physical and mechanical properties of carbide slag soil. In addition, the newly generated CaCO_3 can play the role of surrounding the soil particles and connecting the soil particles, which will increase the cohesion of the soil to a certain extent. This also explains the reason why the strength and cohesion of the modified soil with carbide slag are increased and the disintegration rate and crack rate are decreased from the mineral composition. For tailing sand, with the increase of its ratio, the quartz content gradually increases, which is equivalent to the content of clay minerals gradually decreases (Figure 10c), resulting in the gradual decline of the physical and mechanical properties of the modified soil.

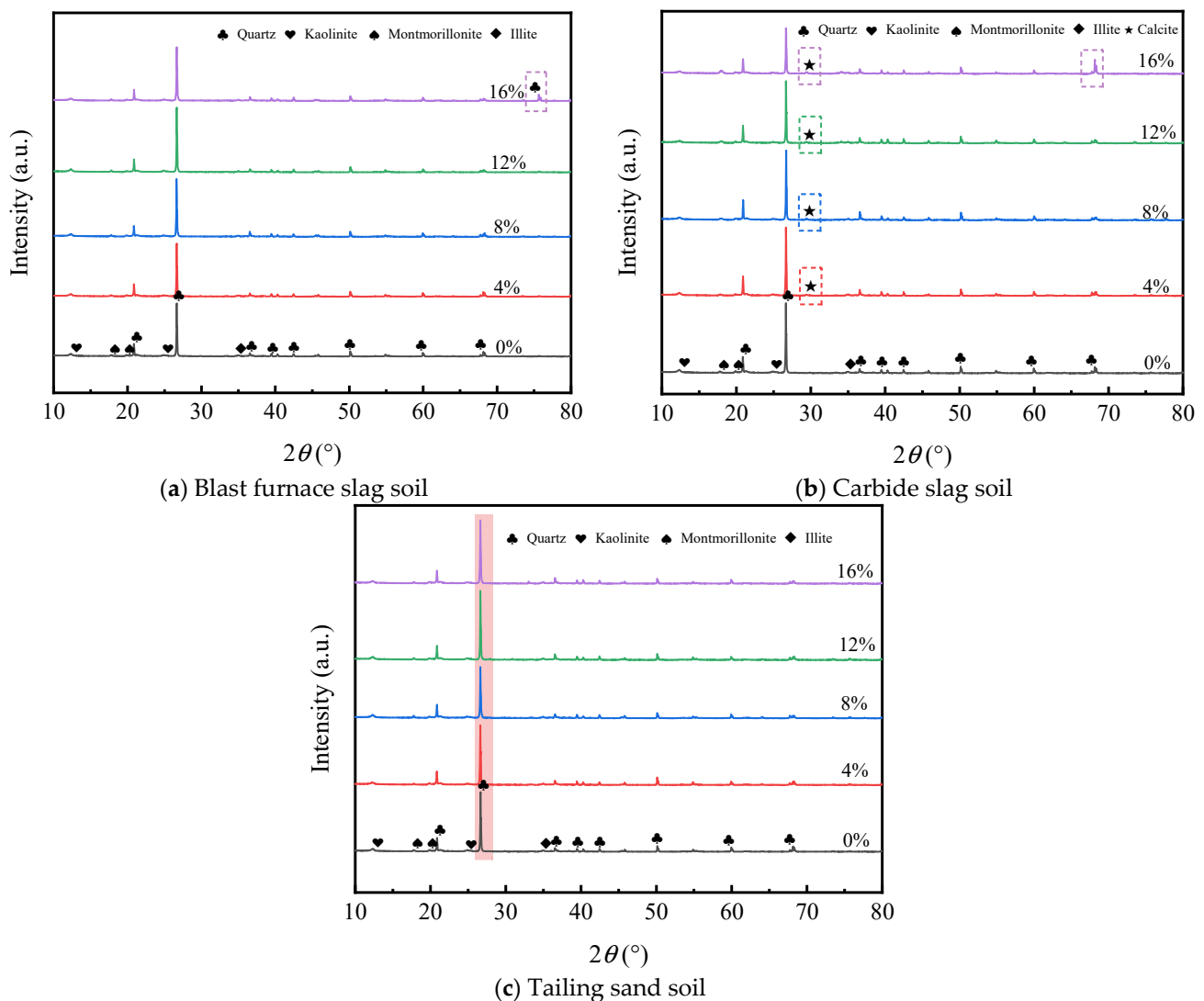


Figure 10. X-ray diffraction patterns of different waste residues soils.

3.8. Microstructure of Different Waste Residues Soils

The first column of Figure 11 is the original SEM map, the second column is the particles and pores distribution map drawn by PCAS software, and the third column is the particle orientation map. In Figure 11a, most of the soil particles in plain soil have smooth surfaces, mainly in the form of surface-to-surface contact, and the distribution of pores is not obvious regularity and there is a certain connectivity between pores. Figure 11b shows the modified soil with a ratio of 16% blast furnace slag. There are many irregular blast furnace slag particles on the soil surface. Because the chemical properties of blast

furnace slag are stable and it is difficult to carry out hydration reaction under the condition of single blast furnace slag, the mechanical strength of soil with single blast furnace slag is not change obviously. Figure 11c shows the modified soil with a ratio of 16% carbide slag. The surface of carbide slag soil particles has tabular crystal, the structure of carbide slag soil gradually becomes compact, and the arrangement and orientation of soil particles are good. Cement such as hydrate (calcium silicate hydrate, calcium aluminate hydrate) and calcium carbonate generated by the reaction between the soil and carbide slag cover the soil particles and connect the adjacent soil particles, which is also the reason that the strength of carbide slag soil increases greatly. Figure 11d shows the soil with a ratio of 16% tailing sand. The surface of the soil particles is rough, and the contact mode is still dominated by surface-to-surface contact. The pore development of the soil is relatively loose after the tailing sand is mixed into the soil, which is also the reason why the strength of the soil decreases after the high liquid limit soil is mixed with the tailing sand.

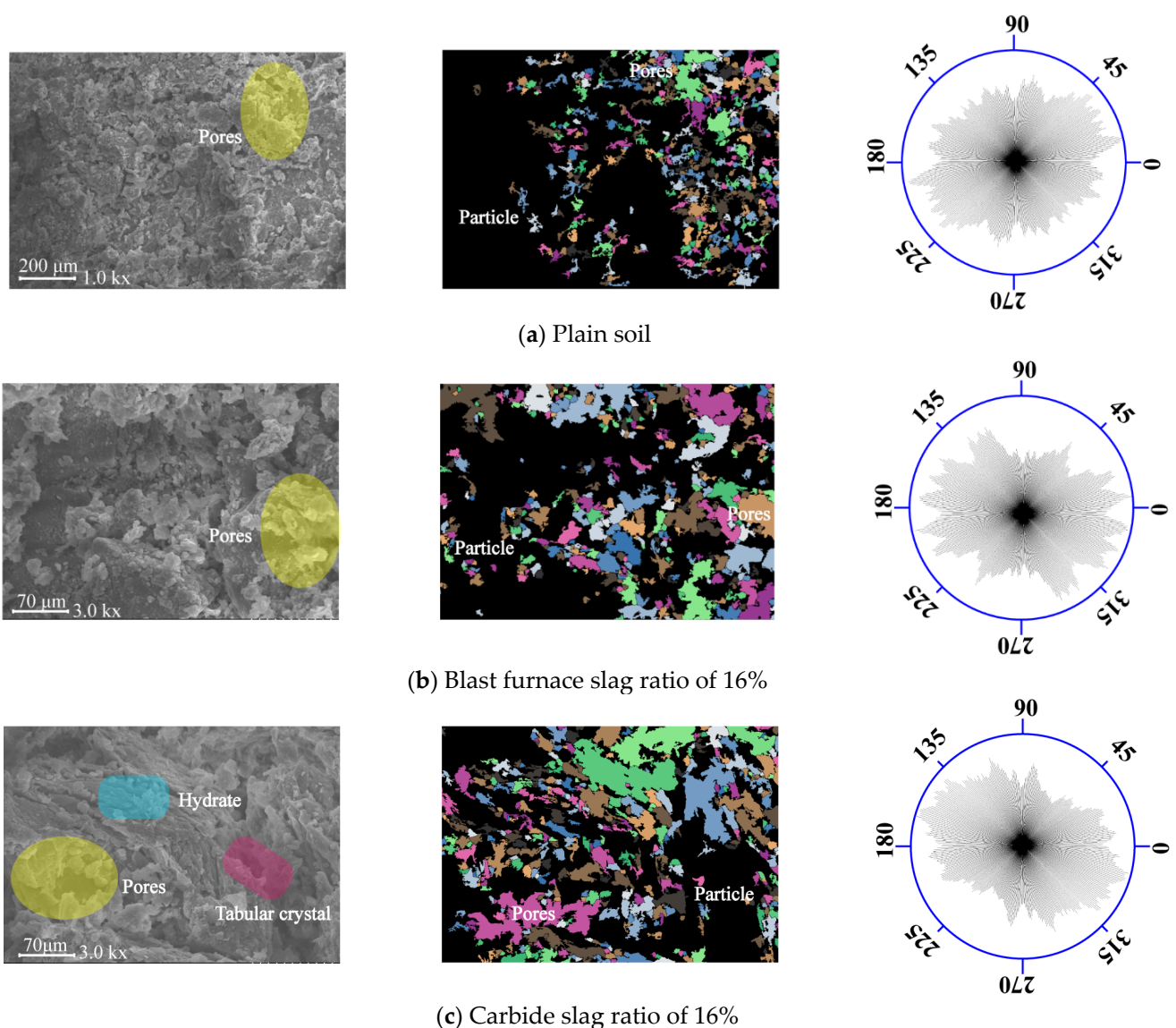
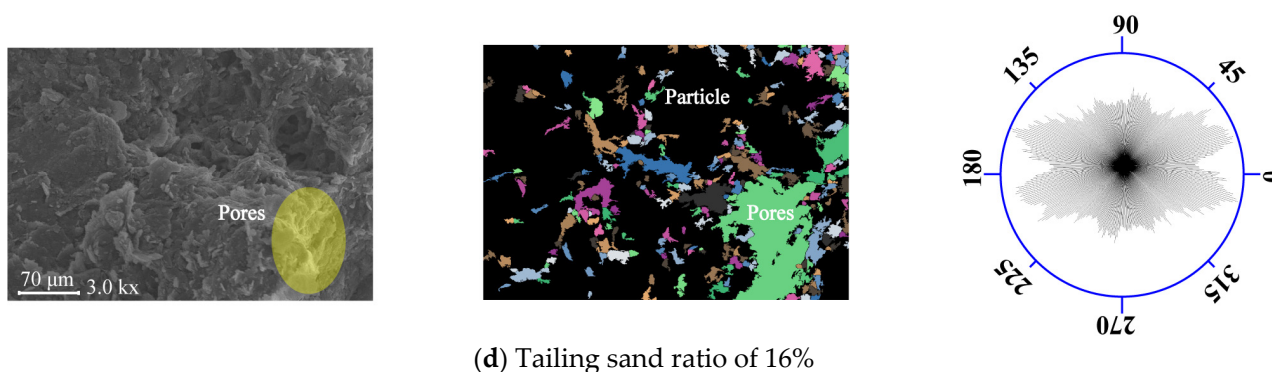


Figure 11. Cont.



(d) Tailing sand ratio of 16%

Figure 11. SEM microstructures of different waste residue soils.

4. Improvement Mechanism and Optimal Ratio of Waste Residues Soils

Figure 12 shows that the improvement mechanism of different waste residues soils is not consistent. The single carbide slag belongs to chemical improvement, so it has the best effect on soil improvement. When carbide slag is added to soil, volcanic ash reactions, carbonation reactions and cation exchange mainly occur. In terms of mineral composition, the volcanic ash and carbonation reactions generate calcium silicate hydrate, calcium aluminate hydrate, and calcium carbonate, and these cements increase the strength of the soil [50,51]. At the same time, the volcanic ash reaction will consume part of the water, and the high liquid limit soil itself has the characteristic of high strength when the water content is low, which will further increase the strength of the soil. In addition, Ca^{2+} in carbide slag can exchange cation with K^+ and Na^+ in high liquid limit soil to compress the electric double layer of high liquid limit soil, which also leads to the improvement of soil strength. In terms of microstructure, due to the compression of the electric double layer of the soil, the pores between the soil will also be reduced, which is also the reason for the increase of the strength of the modified soil. Single-tailing sand belongs to physical improvement, and its improvement effect is not as good as chemical improvement. The obvious edges and corners of tailing sand make the occlusal effect between particles larger, thus increasing the internal friction angle of soil. The increase of the ratio of tailing sand in the soil represents the decrease of the proportion of clay minerals in the soil, which leads to the decrease of its cohesion. Because of a relatively stable protective film on the surface of single blast furnace slag, it is difficult to produce hydration reaction with soil, which can be approximated as physical improvement.

Carbide slag has the best improvement effect among the three kinds of industrial waste residues. Therefore, the relationship between different ratios of carbide slag in high liquid limit soil and various physical and mechanical indexes is studied. As shown in Figure 13, with the increase of carbide slag ratio, the free expansion rate, final disintegration rate, and crack rate of the modified soil all decrease, while the unconfined compressive strength, cohesion and internal friction angle all increase. It can be found that the cohesion of modified soil has the strongest correlation with other physical and mechanical parameters. It can be concluded that cohesion is very important to the improvement of high liquid limit soil. The cohesion of the modified soil is positively correlated with unconfined compressive strength, and internal friction angle, and negatively correlated with free expansion rate, final disintegration rate, and crack rate. According to the relationship between the ratio of carbide slag and the normalized physical and mechanical parameters in Figure 13b, the changes of physical and mechanical parameters of the modified soil with the increase of the ratio of carbide slag can be judged. According to the inflection point in Figure 13b, the optimal ratio of 8% carbide slag in high liquid limit soil is considered comprehensively considering the cost and improvement effect.

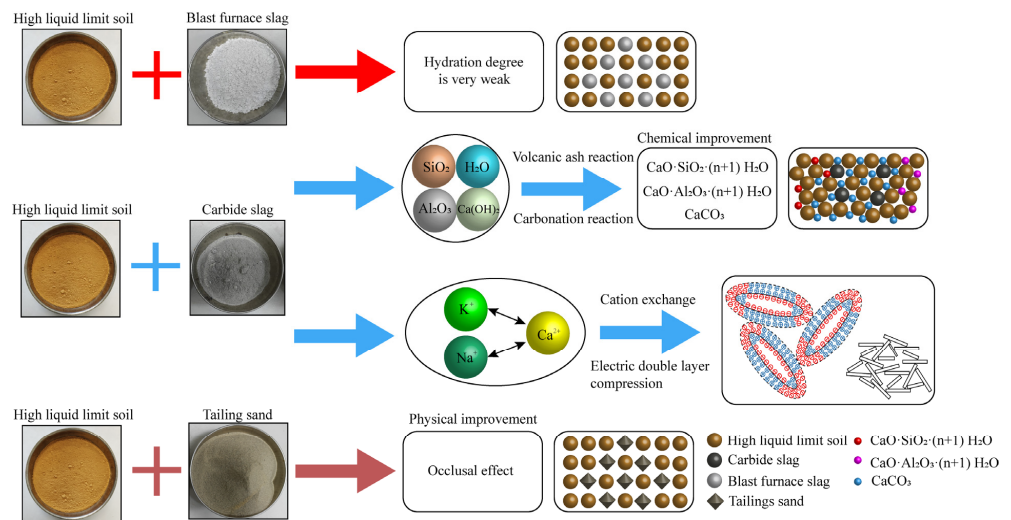
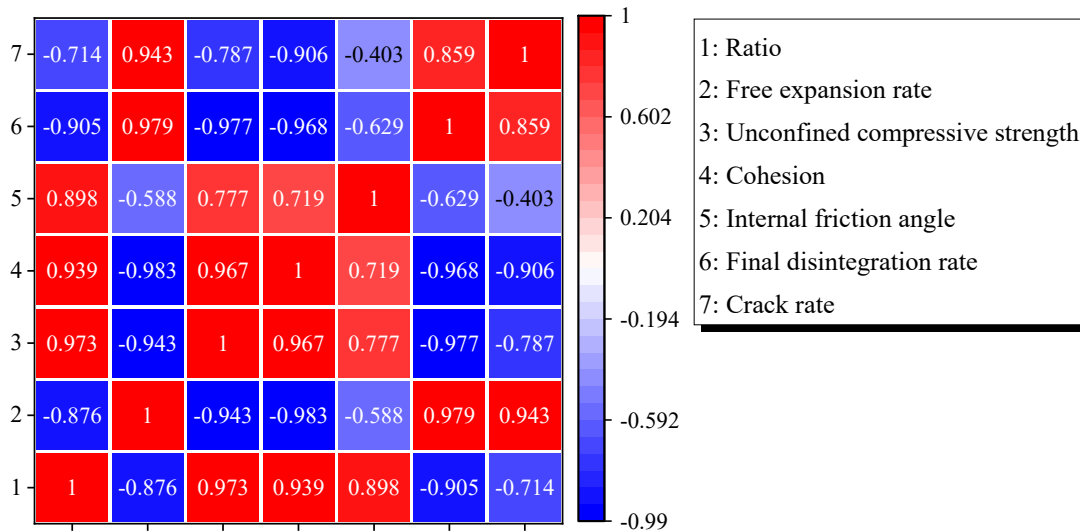
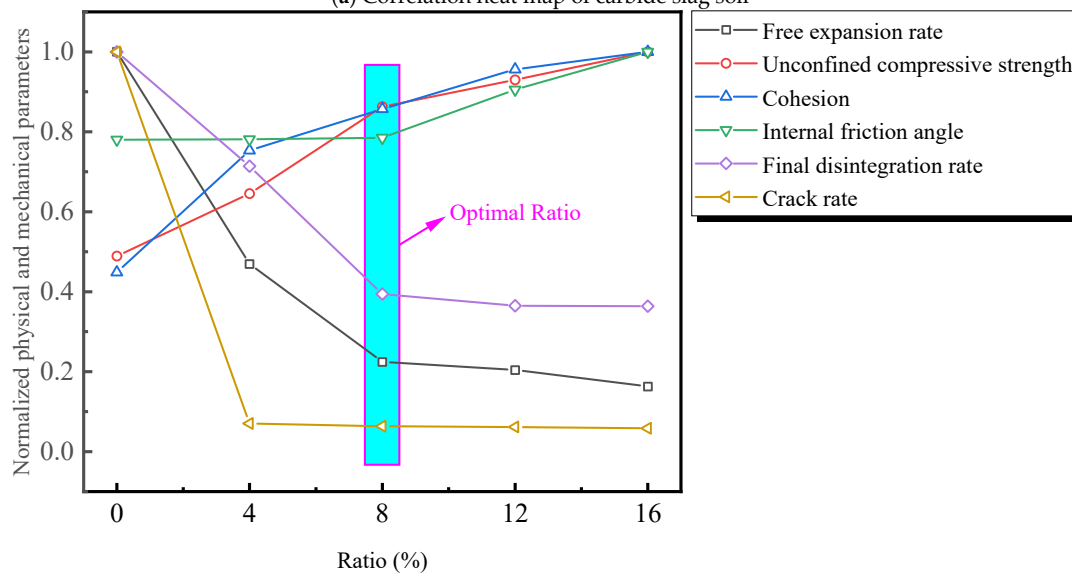


Figure 12. Improvement mechanism of different industrial waste residues soils.



(a) Correlation heat map of carbide slag soil



(b) Normalized physical and mechanical parameters of carbide slag soil with different ratios

Figure 13. Response characteristics of physical and mechanical parameters of carbide slag soil.

5. Conclusions

In this paper, the effects of blast furnace slag, carbide slag, and tailing sand on the engineering characteristics of high liquid limit soil are investigated through experiments. The three kinds of industrial waste residues have different effects on the improvement of high liquid limit soil. The main conclusions are as follows:

- (1) The effect of single blast furnace slag on soil improvement is not obvious. With the increase of the ratio of blast furnace slag, the free expansion rate of soil decreases, and the unconfined compressive strength peaks at 12% after improvement. The change law of cohesion, internal friction angle, and crack rate of modified soil with different ratio of blast furnace slag is not obvious. The greater the ratio of blast furnace slag, the stronger the disintegration of soil sample. Only the free expansion rate and unconfined compressive strength of high liquid limit soil were modified in beneficial direction by single blast furnace slag. Therefore, it is considered that the improvement of single addition of blast furnace slag has both positive and negative effects.
- (2) The effect of single-tailing sand on soil improvement is not obvious. With the increase of tailing sand ratio, the free expansion rate, unconfined compressive strength, cohesion, and crack rate of soil decrease, and the internal friction angle and disintegration rate of soil increase. Only the free expansion rate and crack rate of high liquid limit soil were modified in beneficial direction by single tailing sand. Therefore, it is considered that there are positive effects and negative effects in the improvement of single tailing.
- (3) The single-carbide slag has the best effect on soil improvement and provides better improvement for all the bad engineering properties of high liquid limit soil. With the increase of carbide slag ratio, the free expansion rate, disintegration rate, and crack rate of soil all decrease, while the unconfined compressive strength, cohesion, and internal friction angle all increase. Therefore, it is considered that the improvement of single-calcium carbide slag is a positive effect. Considering the cost and improvement effect, it is considered that 8% ratio of carbide slag is the optimal ratio for improving high liquid limit soil.
- (4) Volcanic ash reaction, carbonation reaction and cation exchange mainly occur in the soil with single-carbide slag, and the generated cement will reduce the porosity of the soil, which leads to the increase of soil strength. The single addition of tailing sand belongs to physical improvement, and the improvement effect is not as good as chemical improvement. The corner angle of tailing sand obviously makes the occlusion between particles greater, thus increasing the internal friction angle of soil. Due to the existence of a relatively stable protective film on the surface of blast furnace slag alone, it is difficult for it to react with the soil in hydration, which can be approximated to physical improvement.

Author Contributions: L.T.: Conceptualization, methodology, writing, revise. Y.C.: Methodology, analysis, writing. J.P.: Experiment, analysis. Z.C.: Check. All authors contributed critically to the drafts and gave final approval for publication. All authors have read and agreed to the published version of the manuscript.

Funding: This research was funded by the National Natural Science Foundation of China (42277142, 41877229, 42102303), Guangdong Basic and Applied Basic Research Foundation (2018B030311066).

Data Availability Statement: Not applicable.

Acknowledgments: The authors are grateful to the anonymous reviewers for their helpful comments on the manuscript.

Conflicts of Interest: The authors declare that they have no conflict of interest.

References

1. Lu, Z.; Fang, R.; Zhan, Y.X.; Yao, H.L. Study on the Dynamic Deformation of Road High Liquid Limit Subgrade Soil. *Adv. Civ. Eng.* **2019**, *2019*, 4084983. [[CrossRef](#)]
2. Yuan, B.X.; Li, Z.H.; Chen, W.J.; Zhao, J.; Lv, J.B.; Song, J.; Cao, X.D. Influence of Groundwater Depth on Pile–Soil Mechanical Properties and Fractal Characteristics under Cyclic Loading. *Fractal Fract.* **2022**, *6*, 198. [[CrossRef](#)]
3. Que, Y.; Lin, Y.Q.; Gong, F.Z. Experimental Study on the Performance of Compound Improved HLLS (High Liquid Limit Soil) with Various Curing Agents. *Key Eng. Mater.* **2017**, *753*, 300–304. [[CrossRef](#)]
4. Yuan, B.X.; Chen, W.J.; Zhao, J.; Li, L.J.; Liu, F.; Guo, Y.C.; Zhang, B.F. Addition of Alkaline Solutions and Fibers for the Reinforcement of Kaolinite-Containing Granite Residual Soil. *Appl. Clay Sci.* **2022**, *228*, 106644. [[CrossRef](#)]
5. Yuan, B.X.; Chen, W.J.; Zhao, J.; Yang, F.; Luo, Q.Z.; Chen, T.Y. The Effect of Organic and Inorganic Modifiers on the Physical Properties of Granite Residual Soil. *Adv. Mater. Sci. Eng.* **2022**, *2020*, 9542258. [[CrossRef](#)]
6. Yan, J.B.; Zou, Z.X.; Mu, R.; Hu, X.L.; Zhang, J.C.; Zhang, W.; Su, A.J.; Wang, J.G.; Luo, T. Evaluating the stability of Outang landslide in the Three Gorges Reservoir area considering the mechanical behavior with large deformation of the slip zone. *Nat. Hazards* **2022**, *112*, 2523–2547. [[CrossRef](#)]
7. Yang, B.B.; Yuan, S.C.; Shen, Z.Z.; Zhao, X.M. Influence of Geotextile Materials on the Fractal Characteristics of Desiccation Cracking of Soil. *Fractal Fract.* **2022**, *6*, 628. [[CrossRef](#)]
8. Yang, B.X.; Chen, M.J.; Chen, W.J.; Luo, Q.Z.; Li, H.Z. Effect of Pile–Soil Relative Stiffness on Deformation Characteristics of the Laterally Loaded Pile. *Adv. Mater. Sci. Eng.* **2022**, *2022*, 4913887. [[CrossRef](#)]
9. Wang, L.; Li, G.X.; Li, X.; Guo, F.X.; Tang, S.W.; Lu, X.; Hanif, A. Influence of reactivity and dosage of MgO expansive agent on shrinkage and crack resistance of face slab concrete. *Cem. Conc. Compos.* **2022**, *126*, 104333. [[CrossRef](#)]
10. Wu, J.; Liu, L.; Deng, Y.F.; Zhang, G.P.; Zhou, A.N.; Xiao, H.L. Use of Recycled Gypsum in the Cement-Based Stabilization of Very Soft Clays and Its Micro-Mechanism. *J. Rock Mech. Geotech.* **2022**, *14*, 909–921. [[CrossRef](#)]
11. Golhashem, M.R.; Uygur, E. Volume Change and Compressive Strength of An Alluvial Soil Stabilized with Butyl Acrylate and Styrene. *Constr. Build. Mater.* **2020**, *255*, 119352. [[CrossRef](#)]
12. Shen, Y.S.; Tang, Y.; Yin, J.; Li, M.P.; Wen, T. An Experimental Investigation on Strength Characteristics of Fiber-Reinforced Clayey Soil Treated with Lime or Cement. *Constr. Build. Mater.* **2021**, *294*, 123537. [[CrossRef](#)]
13. Hou, Y.F.; Li, P.; Wang, J.D. Review of Chemical Stabilizing Agents for Improving the Physical and Mechanical properties of Loess. *Bull. Eng. Geol. Environ.* **2021**, *80*, 9201–9215. [[CrossRef](#)]
14. Develioglu, I.; Pulat, H.F. Shear Strength of Alluvial Soils Reinforced with PP Fibers. *Bull. Eng. Geol. Environ.* **2021**, *80*, 9237–9248. [[CrossRef](#)]
15. Huang, Y.; Wang, L. Experimental Studies on Nanomaterials for Soil Improvement: A Review. *Environ. Earth Sci.* **2016**, *75*, 497. [[CrossRef](#)]
16. Naskar, J.; Chowdhury, S.; Adhikary, A.; Pal, S.; Kazy, S.K. Strength Enhancement of Lateritic Soil Through Mechanical Mixing with Magnetite Nanoparticles, Starch Solution, and Calcite Precipitating Bacteria. *Arab. J. Geosci.* **2021**, *14*, 1901. [[CrossRef](#)]
17. Huang, Y.F.; Fan, W.F.; Wu, J.L.; Xiang, X.L.; Wang, G. Experimental Study on Strength and Microstructure of Glacial Till Stabilized by Ionic Soil Stabilizer. *Buildings* **2022**, *12*, 1446. [[CrossRef](#)]
18. Wang, L.; Zeng, X.M.; Li, Y.; Yang, H.M.; Tang, S.W. Influences of MgO and PVA Fiber on the Abrasion and Cracking Resistance, Pore Structure and Fractal Features of Hydraulic Concrete. *Fractal Fract.* **2022**, *6*, 674. [[CrossRef](#)]
19. Teng, F.; Sie, Y.C.; Ouedraogo, C. Strength Improvement in Silty Clay by Microbial-Induced Calcite Precipitation. *Bull. Eng. Geol. Environ.* **2021**, *80*, 6359–6371. [[CrossRef](#)]
20. Soldo, A.; Miletić, M. Study on Shear Strength of Xanthan Gum-Amended Soil. *Sustainability* **2019**, *11*, 6142. [[CrossRef](#)]
21. Farroukh, H.; Mnif, T.; Kamoun, F.; Kamoun, L.; Bennour, F. Stabilization of Clayey Soils with Tunisian Phosphogypsum: Effect on Geotechnical Properties. *Arab. J. Geosci.* **2018**, *11*, 760. [[CrossRef](#)]
22. Wang, L.; Huang, Y.J.; Zhao, F.; Huo, T.T.; Chen, E.; Tang, S.W. Comparison Between the Influence of Finely Ground Phosphorous Slag and Fly Ash on Frost Resistance, Pore Structures and Fractal Features of Hydraulic Concrete. *Fractal Fract.* **2022**, *6*, 598. [[CrossRef](#)]
23. Wang, L.; Zhou, S.H.; Shi, Y.; Huang, Y.J.; Zhao, F.; Huo, T.T.; Tang, S.W. The Influence of Fly Ash Dosages on the Permeability, Pore Structure and Fractal Features of Face Slab Concrete. *Fractal Fract.* **2022**, *6*, 476. [[CrossRef](#)]
24. Wang, L.; Yu, Z.Q.; Liu, B.; Zhao, F.; Tang, S.W.; Jin, M.M. Effects of Fly Ash Dosage on Shrinkage, Crack Resistance and Fractal Characteristics of Face Slab Concrete. *Fractal Fract.* **2022**, *6*, 335. [[CrossRef](#)]
25. Maghomi, A.; Bakhtiari, M.; Heidari, M. Stabilization and Improvement Soils Characteristics Using Natural and Industrial Additives. *Bull. Eng. Geol. Environ.* **2022**, *81*, 218. [[CrossRef](#)]
26. Odeh, N.A.; Al-Rkaby, A.H.J. Strength, Durability, And Microstructures Characterization of Sustainable Geopolymer Improved Clayey Soil. *Case Stud. Constr. Mat.* **2022**, *16*, e00988. [[CrossRef](#)]
27. Amulya, G.; Moghal, A.A.B.; Basha, B.M.; Basha, B.M.; Almajed, A. Coupled Effect of Granite Sand and Calcium Lignosulphonate on the Strength Behavior of Cohesive Soil. *Buildings* **2022**, *12*, 1687. [[CrossRef](#)]
28. Ma, J.; Yu, Z.Q.; Ni, C.X.; Shi, H.; Shen, X.D. Effects of Limestone Powder on the Hydration and Microstructure Development of Calcium Sulphoaluminate Cement Under Long-Term Curing. *Constr. Build. Mater.* **2019**, *199*, 688–695. [[CrossRef](#)]

29. Ardakani, S.B.; Rajabi, A.M. Laboratory Investigation of Clayey Soils Improvement Using Sepiolite as An Additive; Engineering Performances and Micro-Scale Analysis. *Eng. Geol.* **2021**, *293*, 106328. [[CrossRef](#)]
30. Mahmoudian, H.; Hashemi, M.; Ajalloeian, R.; Movahedi, B. Investigating the Effect of Additives' Size on The Improvement of the Tensile and Compressive Strengths and Deformation Characteristics of Collapsible Soils. *Environ. Earth Sci.* **2020**, *79*, 328. [[CrossRef](#)]
31. Kong, X.H.; Wang, G.Q.; Liang, Y.P.; Zhang, Z.B.; Cui, S. The Engineering Properties and Microscopic Characteristics of High-Liquid-Limit Soil Improved with Lignin. *Coatings* **2022**, *12*, 268. [[CrossRef](#)]
32. Sun, Y.L.; Liu, Q.X.; Xu, H.S.; Wang, Y.X.; Tang, L.S. Influences of Different Modifiers on the Disintegration of Improved Granite Residual Soil Under Wet and Dry Cycles. *Int. J. Min. Sci. Technol.* **2022**, *32*, 831–845. [[CrossRef](#)]
33. Wang, S.N.; Chen, F.Y.; Xue, Q.P.; Zhang, P. Splitting Tensile Strength of Cement Soil Reinforced with Basalt Fibers. *Materials* **2020**, *13*, 3110. [[CrossRef](#)] [[PubMed](#)]
34. Ghadakpour, M.; Choobasti, A.J.; Kutanaei, S.S. Experimental Study of Impact of Cement Treatment on the Shear Behavior of Loess and Clay. *Arab. J. Geosci.* **2020**, *13*, 184. [[CrossRef](#)]
35. Bagriacik, B. Utilization of Alkali-Activated Construction Demolition Waste for Sandy Soil Improvement with Large-Scale Laboratory Experiments. *Constr. Build. Mater.* **2021**, *302*, 124173. [[CrossRef](#)]
36. de Araujo, M.T.; Ferrazzo, S.T.; Bruschi, G.J.J.; Consoli, N.C. Mechanical and Environmental Performance of Eggshell Lime for Expansive Soils Improvement. *Transp. Geotech.* **2021**, *31*, 100681. [[CrossRef](#)]
37. Ma, J.R.; Su, Y.H.; Liu, Y.Y.; Tao, X.L. Strength and Microfabric of Expansive Soil Improved with Rice Husk Ash And Lime. *Adv. Civ. Eng.* **2020**, *2020*, 9646205. [[CrossRef](#)]
38. Benhelal, E.; Zahedi, G.; Shamsaei, E.; Bahadori, A. Global Strategies and Potentials to Curb CO₂ Emissions in Cement Industry. *J. Clean. Prod.* **2013**, *51*, 142–161. [[CrossRef](#)]
39. Tan, T.T.; Huat, B.B.K.; Anggraini, V.; Shukla, S.K.; Nahazanan, H. Strength Behavior of Fly Ash-Stabilized Soil Reinforced with Coir Fibers in Alkaline Environment. *J. Nat. Fibers* **2019**, *18*, 1556–1569. [[CrossRef](#)]
40. Dang, L.C.; Khabbaz, H.; Ni, B.J. Improving Engineering Characteristics of Expansive Soils Using Industry Waste as a Sustainable Application for Reuse of Bagasse Ash. *Transp. Geotech.* **2021**, *31*, 100637. [[CrossRef](#)]
41. Shahsavani, S.; Vakili, A.H.; Mokhberi, M. The Effect of Wetting and Drying Cycles on the Swelling-Shrinkage Behavior of the Expansive Soils Improved by Nanosilica and Industrial Waste. *Bull. Eng. Geol. Environ.* **2020**, *79*, 4765–4781. [[CrossRef](#)]
42. Danish, A.; Totić, E.; Bayram, M.; Sütçü, M.; Gencil, O.; Erdoğan, E.; Ozbakkaloglu, T. Assessment of Mineralogical Characteristics of Clays and the Effect of Waste Materials on Their Index Properties for the Production of Bricks. *Materials* **2022**, *15*, 8908. [[CrossRef](#)] [[PubMed](#)]
43. Zhou, Y.; Liu, W. Application of Granulated Copper Slag in Massive Concrete Under Saline Soil Environment. *Constr. Build. Mater.* **2021**, *266*, 121165. [[CrossRef](#)]
44. Jiang, W.G.; Li, X.G.; Lv, Y.; Jiang, D.B.; Liu, Z.L.; He, C.H. Mechanical and Hydration Properties of Low Clinker Cement Containing High Volume Superfine Blast Furnace Slag and Nano Silica. *Constr. Build. Mater.* **2020**, *238*, 117683. [[CrossRef](#)]
45. Du, Y.J.; Zhang, Y.Y.; Liu, S.Y. Investigation of Strength and California Bearing Ratio Properties of Natural Soils Treated by Calcium Carbide Residue. *Proc. Geo Front.* **2011**, *2011*, 1237–1244. [[CrossRef](#)]
46. Liu, X.Y.; Zhang, X.W.; Kong, L.W.; Wang, G.; Liu, H.H. Formation Mechanism of Collapsing Gully in Southern China and the Relationship with Granite Residual Soil: A Geotechnical Perspective. *Catena* **2022**, *210*, 105890. [[CrossRef](#)]
47. Yang, B.B.; Li, D.D.; Yuan, S.C.; Jin, L.C. Role of Biochar from Corn Straw in Influencing Crack Propagation and Evaporation in Sodic Soils. *Catena* **2021**, *204*, 105457. [[CrossRef](#)]
48. Liu, C.; Tang, C.S.; Shi, B.; Suo, W.B. Automatic Quantification of Crack Patterns by Image Processing. *Comput. Geosci.* **2013**, *57*, 77–80. [[CrossRef](#)]
49. Tang, L.S.; Liu, Q.X.; Sun, Y.L.; Xu, H.S. Water Entrance-And-Release Capacity and Contact Angle of Improved Granite Residual Soil. *Hydrogeol. Eng. Geol.* **2022**, *49*, 144–156. [[CrossRef](#)]
50. Wang, Y.T.; Zhao, H.B.; Degracia, K.; Han, L.X.; Sun, H.; Sun, M.Z.; Wang, Y.Z.; Schiraldi, D.A. Green Approach to Improving the Strength and Flame Retardancy of Poly (Vinyl Alcohol)/Clay Aerogels: Incorporating Biobased Gelatin. *ACS Appl. Mater. Inter.* **2017**, *9*, 42258–42265. [[CrossRef](#)]
51. Sun, M.Z.; Sun, H.; Hostler, S.; Schiraldi, D.A. Effects of Feather-Fiber Reinforcement on Poly (Vinyl Alcohol)/Clay Aerogels: Structure, Property and Applications. *Polymers* **2018**, *137*, 201–208. [[CrossRef](#)]

Disclaimer/Publisher's Note: The statements, opinions and data contained in all publications are solely those of the individual author(s) and contributor(s) and not of MDPI and/or the editor(s). MDPI and/or the editor(s) disclaim responsibility for any injury to people or property resulting from any ideas, methods, instructions or products referred to in the content.